

# Coupling of Current and Flow Relaxation in Reversed-Field Pinches Due to Two-Fluid Effects

C. R. Sovinec,<sup>1</sup> J. R. King,<sup>1,2</sup> J. P. Sauppe,<sup>1</sup>  
V. V. Mirnov,<sup>1</sup> J. S. Sarff,<sup>1</sup> and W. X. Ding<sup>3</sup>

<sup>1</sup>*University of Wisconsin-Madison*

<sup>2</sup>*Tech-X Corporation*

<sup>3</sup>*University of California at Los Angeles*

2012 Fusion Energy Conference

October 8-12, 2012      San Diego, CA



# Objective

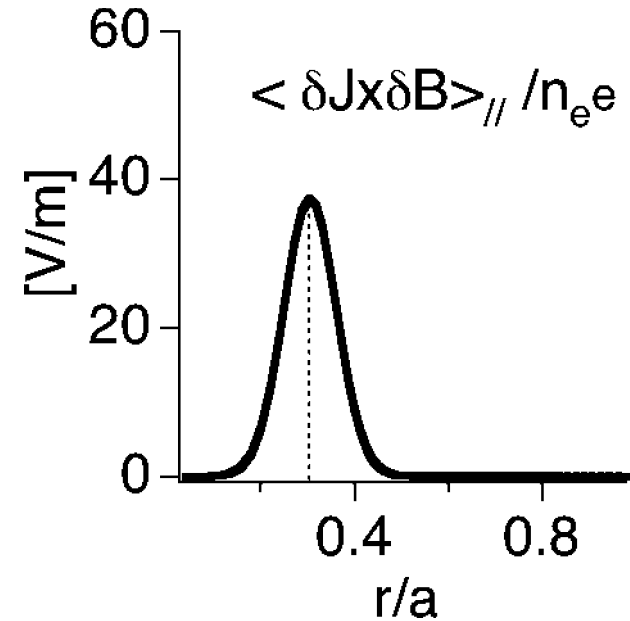
To understand effects that couple current-profile and flow-profile relaxation (momentum transport) during relaxation events in the Madison Symmetric Torus (MST).

# Outline

- Introduction
- Modeling
- Linear results
- Nonlinear island evolution
- Dynamo and momentum transport in multi-helicity relaxation
- Multi-helicity relaxation with background flow
- Discussion and conclusions

## Introduction: Measurements on MST point to the importance of two-fluid effects during relaxation events.

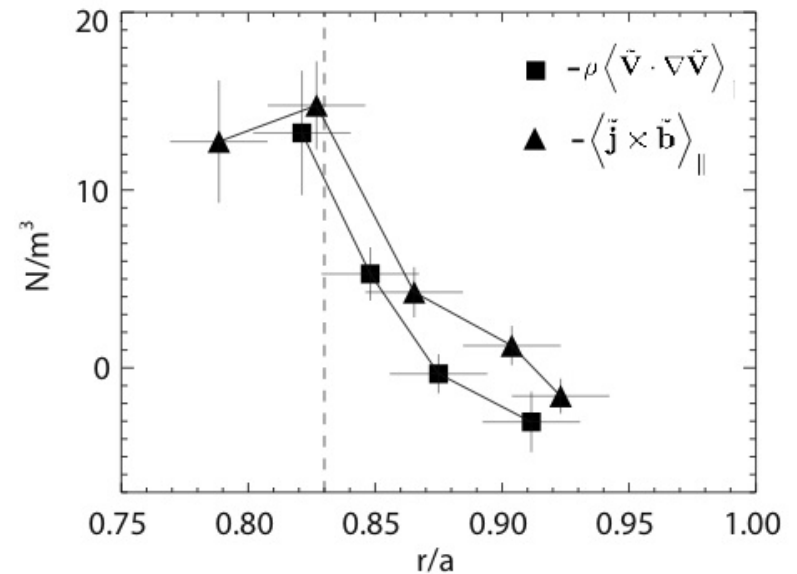
- In standard MST operation, magnetic relaxation occurs during discrete sawtooth events.
- Laser polarimetry measurements of  $\delta j_\phi$  for the (1,6) mode, and fitted  $\delta \mathbf{b}$  profiles show a correlation that implies significant Hall dynamo. [Ding, *et al.*, PoP **13**, 112306].
- MST parameters have ion-sound-gyroradius ( $\rho_s = c_s / \Omega_i$ ) comparable to the resistive skin depth, so two-fluid linear tearing effects are expected [Mirnov, *et al.*, PoP **11**, 4468, for example].



Hall dynamo from (1,6) mode, inferred with multi-chord laser polarimetry measurements on MST.

## Probe measurements from MST's edge plasma also indicate the significance of two-fluid effects.

- The existence of Hall dynamo and net parallel Lorentz force density from fluctuations are essentially equivalent.
- Kuritsyn, *et al.*, used an array of magnetic coil triplets to measure Maxwell-stress profiles in the edge of MST [PoP **16**, 55903].
- The group also found Reynolds stress contributions from flow fluctuations, measured by Mach probes.
- With respect to momentum transport, the effects largely cancel.



**Fluctuation-induced Lorentz and inertial force densities from probe measurements during a relaxation event.**

**Modeling:** We apply two-fluid modeling to investigate these macroscopic RFP dynamics.

$$\frac{\partial n}{\partial t} + \nabla \cdot (n\mathbf{V}) = 0$$

particle continuity

$$mn \left( \frac{\partial}{\partial t} + \mathbf{V} \cdot \nabla \right) \mathbf{V} = \mathbf{J} \times \mathbf{B} - \nabla \sum_{\alpha} n T_{\alpha} - \nabla \cdot \underline{\underline{\Pi}}$$

flow evolution

$$\frac{3}{2} n \left( \frac{\partial}{\partial t} + \mathbf{V}_{\alpha} \cdot \nabla \right) T_{\alpha} = -n T_{\alpha} \nabla \cdot \mathbf{V}_{\alpha} - \nabla \cdot \mathbf{q}_{\alpha} + Q_{\alpha}$$

temperature evolution

$$\frac{\partial \mathbf{B}}{\partial t} = -\nabla \times \left[ \eta \mathbf{J} - \mathbf{V} \times \mathbf{B} + \frac{1}{ne} \mathbf{J} \times \mathbf{B} - \frac{T_e}{ne} \nabla n + \frac{m_e}{ne^2} \frac{\partial}{\partial t} \mathbf{J} \right]$$

Faraday's / Ohm's law

$$\mu_0 \mathbf{J} = \nabla \times \mathbf{B}$$

low- $\omega$  Ampere's law

$$\nabla \cdot \mathbf{B} = 0$$

divergence constraint

- Initial-value computations with the two-fluid system are solved using the NIMROD code [JCP **229**, 5803 (2010)].

The closure for stress ( $\underline{\Pi}$ ) is a combination of Braginskii ion gyroviscosity and isotropic viscous stress.

$$\underline{\Pi}_{\text{gv}} = \frac{m_i p_i}{4eB} \left[ \hat{\mathbf{b}} \times \underline{\mathbf{W}} \cdot (\underline{\mathbf{I}} + 3\hat{\mathbf{b}}\hat{\mathbf{b}}) - (\underline{\mathbf{I}} + 3\hat{\mathbf{b}}\hat{\mathbf{b}}) \cdot \underline{\mathbf{W}} \times \hat{\mathbf{b}} \right], \quad \left( \underline{\mathbf{W}} \equiv \nabla \mathbf{V} + \nabla \mathbf{V}^T - \frac{2}{3} \underline{\mathbf{I}} \nabla \cdot \mathbf{V} \right)$$

$$\underline{\Pi}_{\perp} \sim -\frac{3p_i m_i^2}{10e^2 B^2 \tau_i} \underline{\mathbf{W}}, \quad \text{treated as } -nm_i \nu_{iso} \underline{\mathbf{W}}$$

The computations presented here have finite but uniform background pressure, representing conditions in the RFP core without detailed transport modeling.

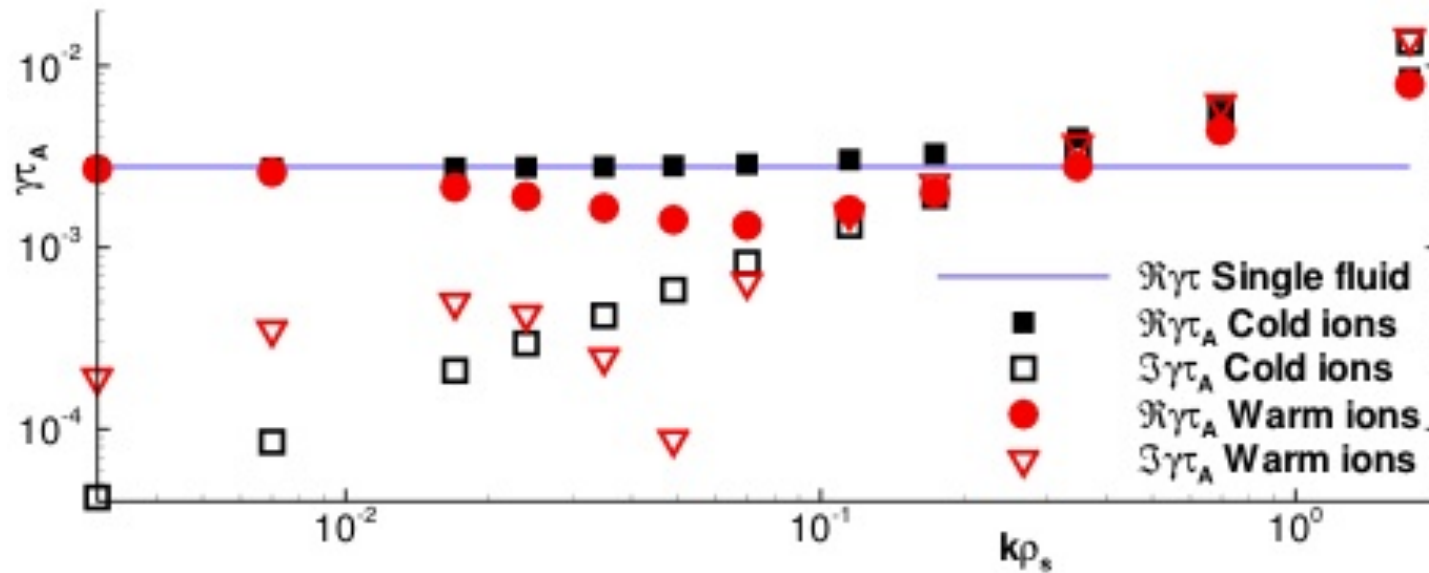
$$\mathbf{q} = -n\chi_{iso} \nabla T$$

## Linear results: ‘Fast tearing’ was expected, a slower intermediate regime was not.

- Analytical asymptotic results for linear tearing in a slab with uniform equilibrium pressure finds  $\gamma > \gamma_{MHD}$  for  $\rho_s > \delta$ . [Mirnov; also Ahedo and Ramos, PPCF **51**, 55018.]
- Our linear slab computations [Sovinec and King, JCP **229**, 5803 (2010)] reproduce the analytics.
- Cold-ion results for paramagnetic pinch equilibria also show growth rates that are larger than resistive-MHD.

	MST	comput.
$\beta$	0.03	0.1
$kd_i$	0.7	0.01-6.0
$k\rho_s$	0.05	0.003-1.7

Warm-ion (gyroviscous,  $T_i = T_e$ ) results for cylindrical geometry find  $\gamma < \gamma_{MHD}$  at intermediate  $\rho_s$ -values.



Growth rates (solid) and frequencies (open) from warm-ion (red) and cold-ion (black) computations with NIMROD. [log-log scale]

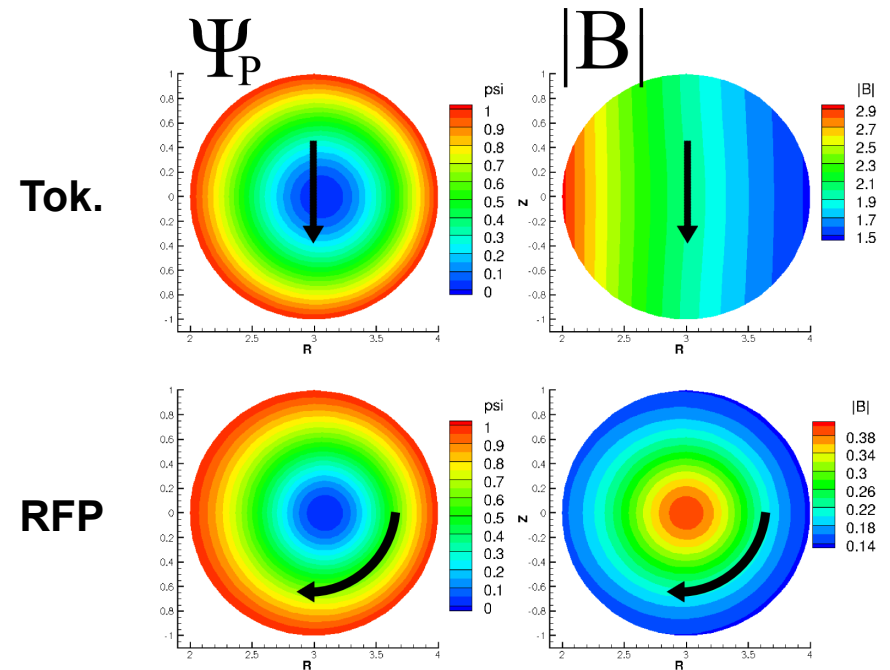
- The effect does not occur for warm-ion computations in slab geometry.



# Our analysis of the ion gyroviscous stress indicates drift-tearing effects from $\nabla B$ and poloidal curvature.

- Expanding  $\hat{\mathbf{b}}_0$  and  $\mathbf{k}$  about the resonance in tearing ordering and analyzing  $2\hat{\mathbf{b}}_0 \times \boldsymbol{\kappa}_0 \cdot \nabla \cdot \tilde{\Pi}$  and  $-\hat{\mathbf{b}}_0 \cdot \nabla \times \nabla \cdot \tilde{\Pi}$  contributions to parallel vorticity evolution finds a drift contribution with frequency [King, *et al.*, PoP **18**, 42303]:

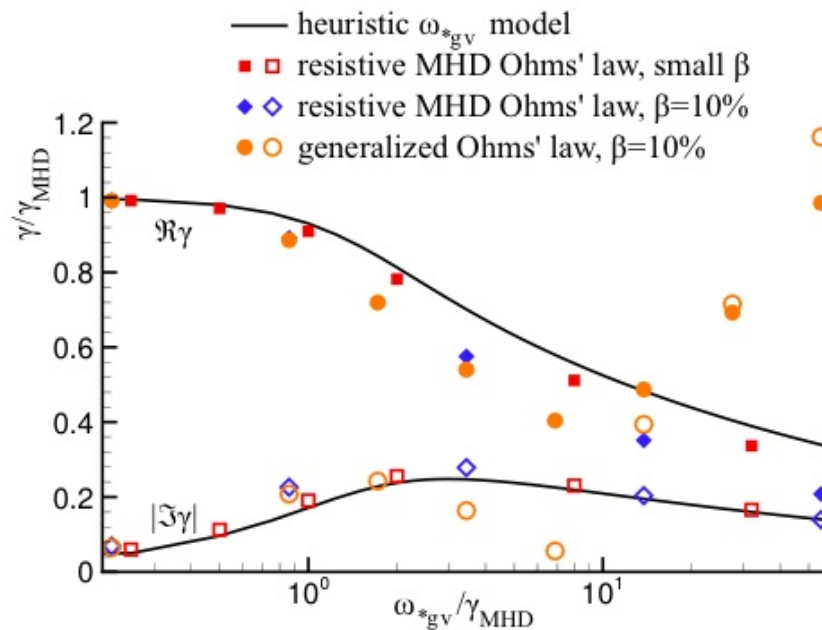
$$\omega_{*gv} = \frac{k_{\perp}}{m_i n_0} \frac{p_{i0}}{\Omega_{i0}} \left( \frac{3}{2r} \frac{B_{\theta 0}^2}{B_0^2} - \frac{B'_0}{B_0} \right)$$



Poloidal flux (left) and  $B$  (right) for tokamaks (top) and RFPs (bottom). Arrows show projections of  $\nabla B$  and curvature drifts.

A simplified model with gyroviscous stress and resistive-MHD Ohm's law reproduces the stabilizing effect.

- The derivation also neglects compressive responses from pressure, and the dispersion relation is just  $\gamma^4 (\gamma - i\omega_{*gv}) = \gamma_{MHD}^5$  .

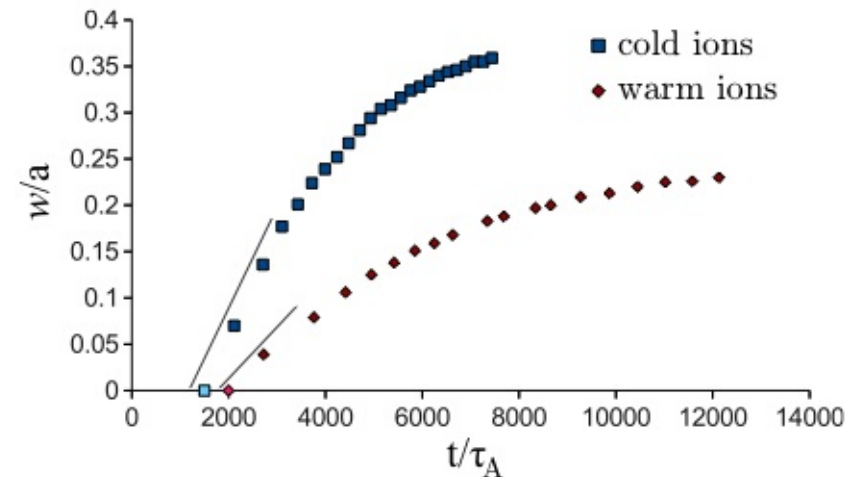


Two-fluid computations and heuristic dispersion relation (drift & resistive-MHD Ohm's law) agree until KAW reconnection is significant,  $\rho_s \sim \delta$ .

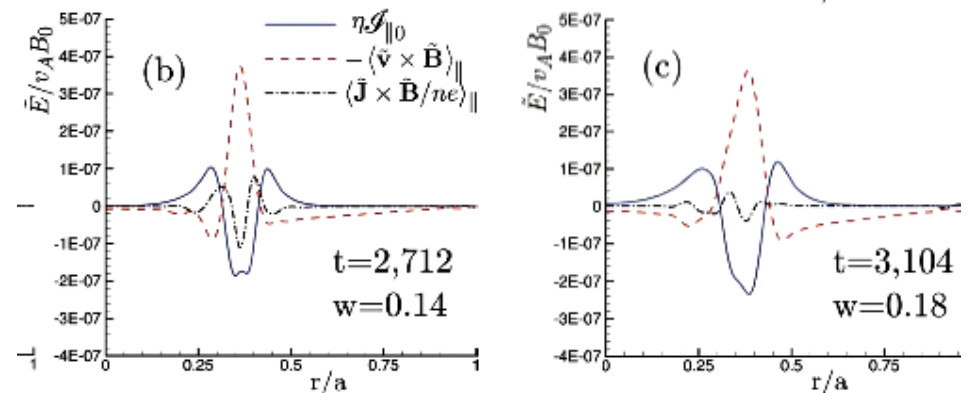
- Warm ions in pinch profiles lead to drift-tearing, even with  $\nabla p_0=0$ .

# Nonlinear single-helicity: Nonlinear island saturation with cold ions matches MHD.

- The computations have  $R/a = 0.51$  to prohibit multi-helicity dynamics.
- Coupling to  $m \neq 1$  components is allowed but is not significant in the results.
- We observe that island evolution reverts to MHD dynamics, i.e. vanishing Hall effect, when the island width exceeds the ion skin depth.



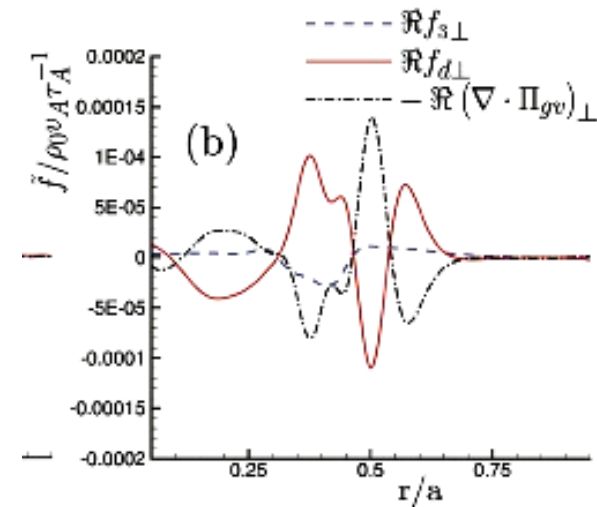
Island-width evolution shows a Rutherford stage for cold and warm ions.



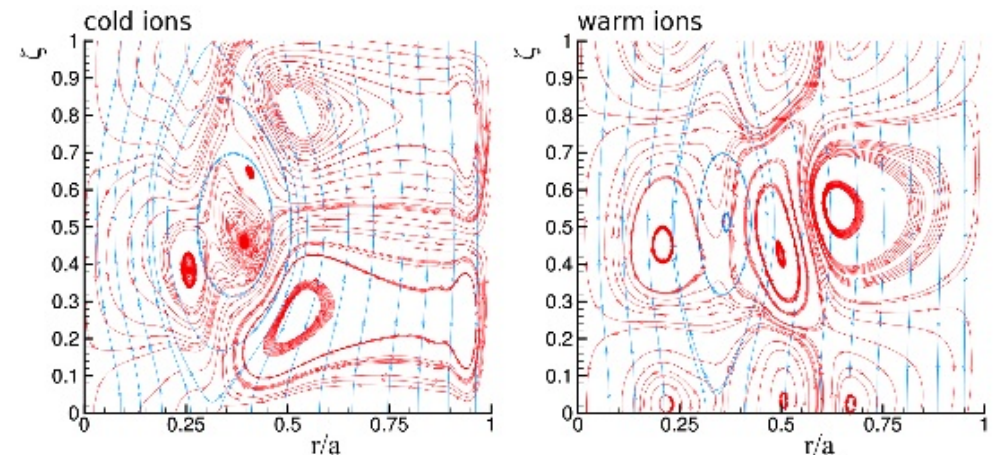
Hall dynamo effect in cold-ion evolution vanishes when  $w$  exceeds  $d_i$  (0.17a).

## With warm ions, saturation occurs at smaller width.

- Forces from gyroviscous stress supplement Rutherford's 3rd-order Lorentz force to balance the 1st-order drive.
- The important gv forces result from flows that are out of phase with the standard reconnection flow pattern.
- The out-of-phase flows are influenced by Lorentz forces from perturbed currents resulting from electron-ion decoupling (Hall effect).
- The flows are insensitive to S and viscous dissipation.
- Unlike tokamak diamagnetic drift-tearing, transport does not eliminate large-w FLR [King, PoP **18**, 42303].



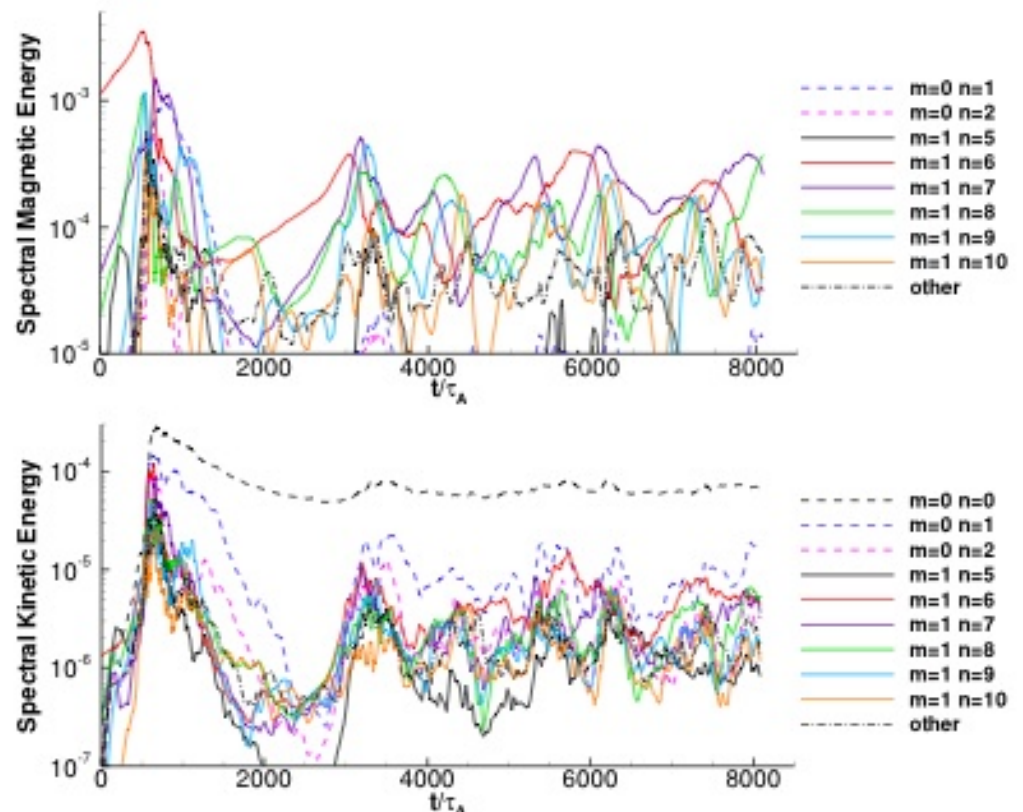
**Comparison of 3rd-order, 1st-order, and gyroviscous forces at saturation.**



**Saturated helical flow streamtraces show different phases for cold-ion (left) and warm-ion (right) results.**

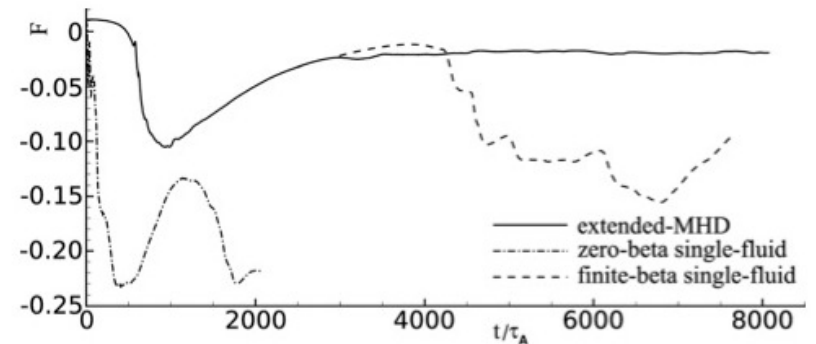
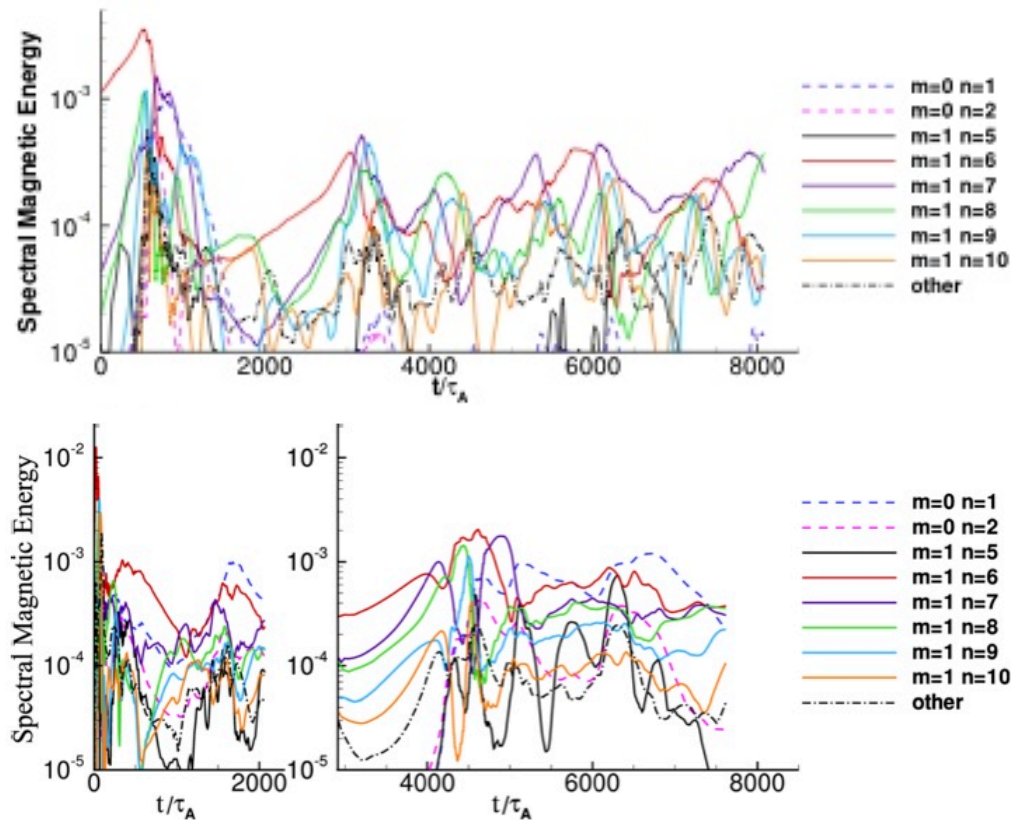
# Nonlinear multi-helicity: Results at realistic $R/a$ are more directly relevant to standard operation.

- Our multi-helicity two-fluid computations have  $R/a=3$  in cylindrical geometry, Hall effect, and gyroviscous stress from warm ions.
- Plasma parameters have  $S=8\times 10^4$ ,  $Pm=1$ ,  $\beta=0.1$ , and  $\rho_s=0.05a$ .
- Overall evolution at  $\Theta=1.6$  shows familiar fluctuation dynamics and field reversal
- Dynamics remain nearly 'force-free.'
- Magnetic energy in  $m=0$  fluctuations is relatively weak after the first event.



Evolution of fluctuation energies in the two-fluid computation.

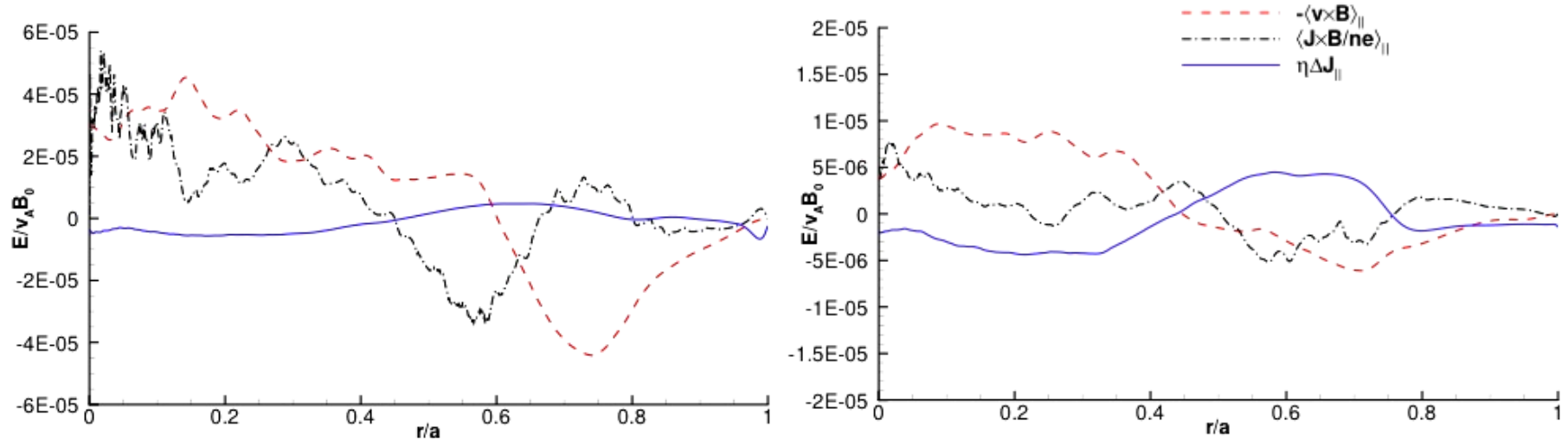
MHD computations of the same conditions have larger core fluctuation amplitudes and more nonlinear coupling.



Smaller fluctuation levels in the two-fluid computation leads to less reversal than in the MHD computations for the same conditions.

MHD computations started at  $t=0$  with  $0-\beta$  (below left) and at later time with finite- $\beta$  (below right) develop larger  $m=0$  fluctuations than the two-fluid model (top).

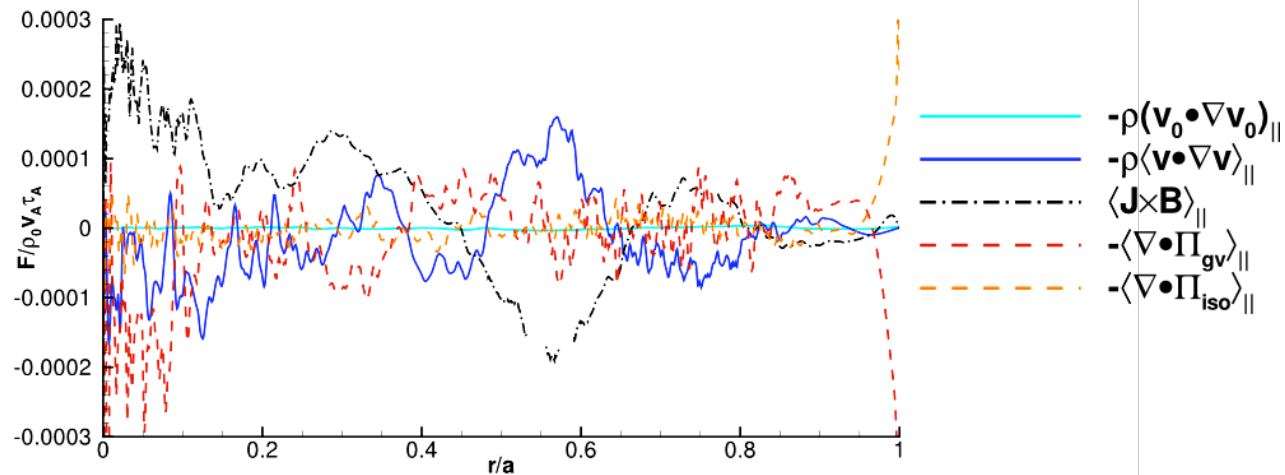
# Two-fluid multi-helicity computations with $(\rho_s/a)$ -values relevant to MST exhibit Hall dynamo during relaxation.



**Hall dynamo is evident and comparable in magnitude to the MHD dynamo during the initial (left) and a subsequent (right) relaxation event.**

- Our computations at ion sound gyroradius  $(c_s/\Omega_i)$   $\rho_s=0.05a$  show significant Hall and MHD dynamo effects that are comparable in magnitude during a relaxation event.
- As in single-fluid computation, the combined dynamo emfs act to reduce parallel current in the core and drive it near the edge.
- Evaluating for MST,  $5 \times 10^{-5} v_A B_0$  is 40 V/m, so the predicted magnitude is comparable to the Hall emf measured by Ding et al. [PRL **93**, 2004].

There is also significant momentum transport during two-fluid relaxation with  $m=0$  mode activity.



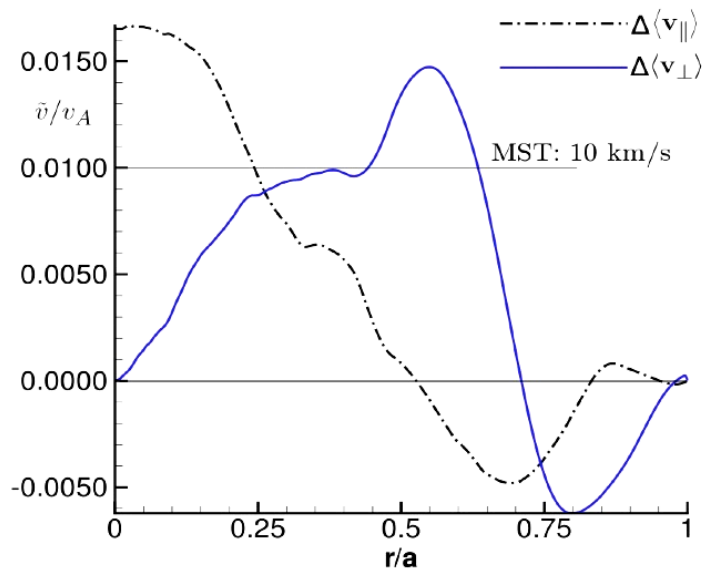
**Force densities that affect simulated net parallel flow during a relaxation event, including contributions from Maxwell stress (black) and Reynolds stress (blue).**

- Simulations show transport of parallel momentum driven by fluctuation-induced forces from Maxwell, Reynolds, and gyroviscous stresses.
- The fluctuation-induced Maxwell stress is linked to the Hall dynamo.
- Similar to measurements by Kuritsyn et al. [Phys. Plasmas **16**, 2009] in the edge of MST, the Maxwell and Reynolds stresses tend to cancel.
- The warm-ion computations also show significant gyroviscous forces.

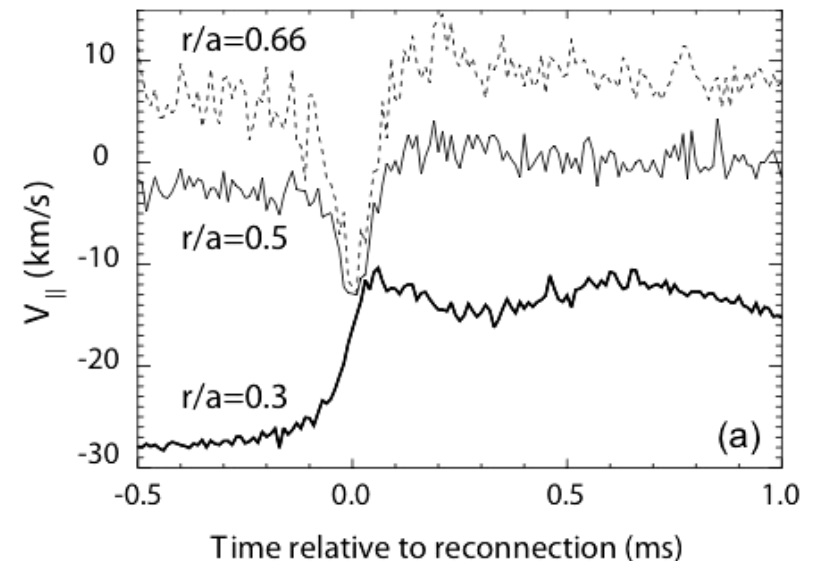


Similar to MST, the large relaxation event increases parallel flow in the core and reduces it near the edge.

- The net change in flow profile is only significant with two-fluid effects.
- These simulations do not include other transport effects that maintain flow profiles.
- The relevance of analytical two-fluid relaxation theory [papers by Steinhauer, Hegna, for example] is intriguing but needs further study.



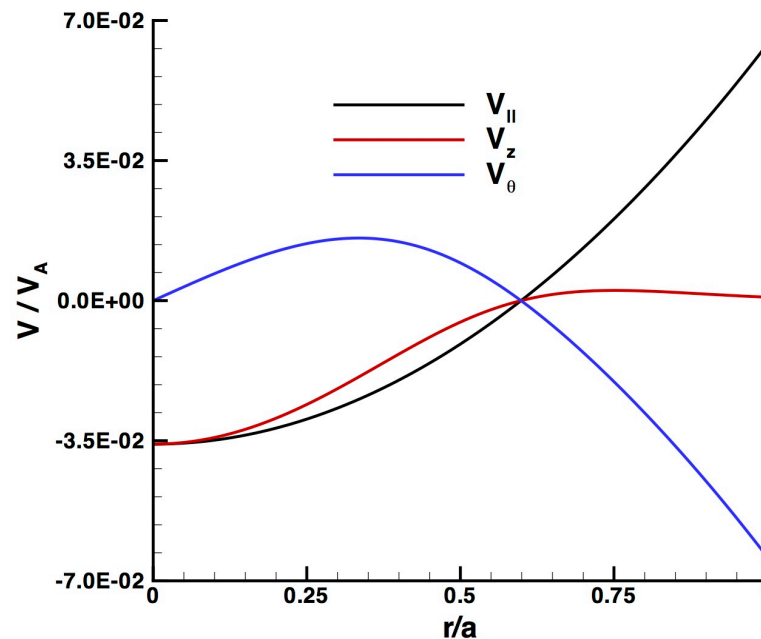
Profiles of parallel (black) and perpendicular (blue) flow generated by the first simulated relaxation event.



Temporal evolution of parallel flow at three radii in MST. [Kuritsyn, PoP 16, 55903]

## Multi-helicity with background flow: MST develops a parallel-flow profile between events.

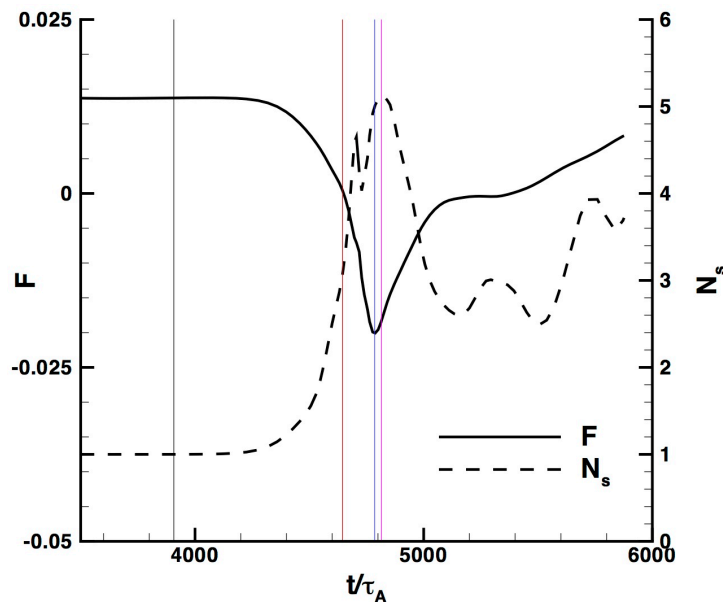
- We use a background parallel-flow profile that matches the experimental measurements between events at the probe locations shown above.
- Computing with  $S=5000$  facilitates scanning different configurations.



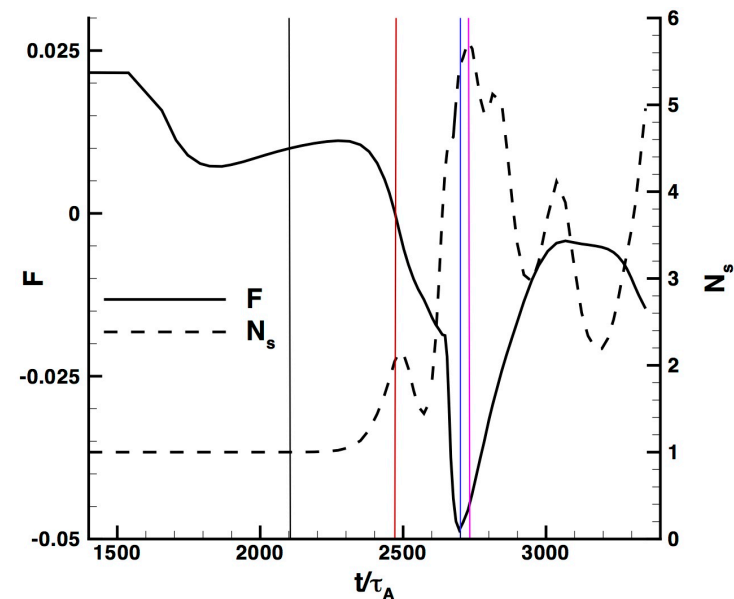
**This background parallel-flow profile is used in all of the following results.**

# Background flow breaks the symmetry of relaxation relative to positive and negative current.

- Results with negative current,  $\mathbf{J}_0 \cdot \mathbf{B}_0 < 0$ , exhibit approximately twice as much field-reversal during the first relaxation event.
- Somewhat more nonlinear coupling occurs, as evident from the larger spectral width,  $N_s \equiv (\sum_n W_{1,n})^2 / \sum_n W_{1,n}^2$ , where  $W_{1,n}$  is the magnetic fluctuation energy in the  $(m=1,n)$  component.



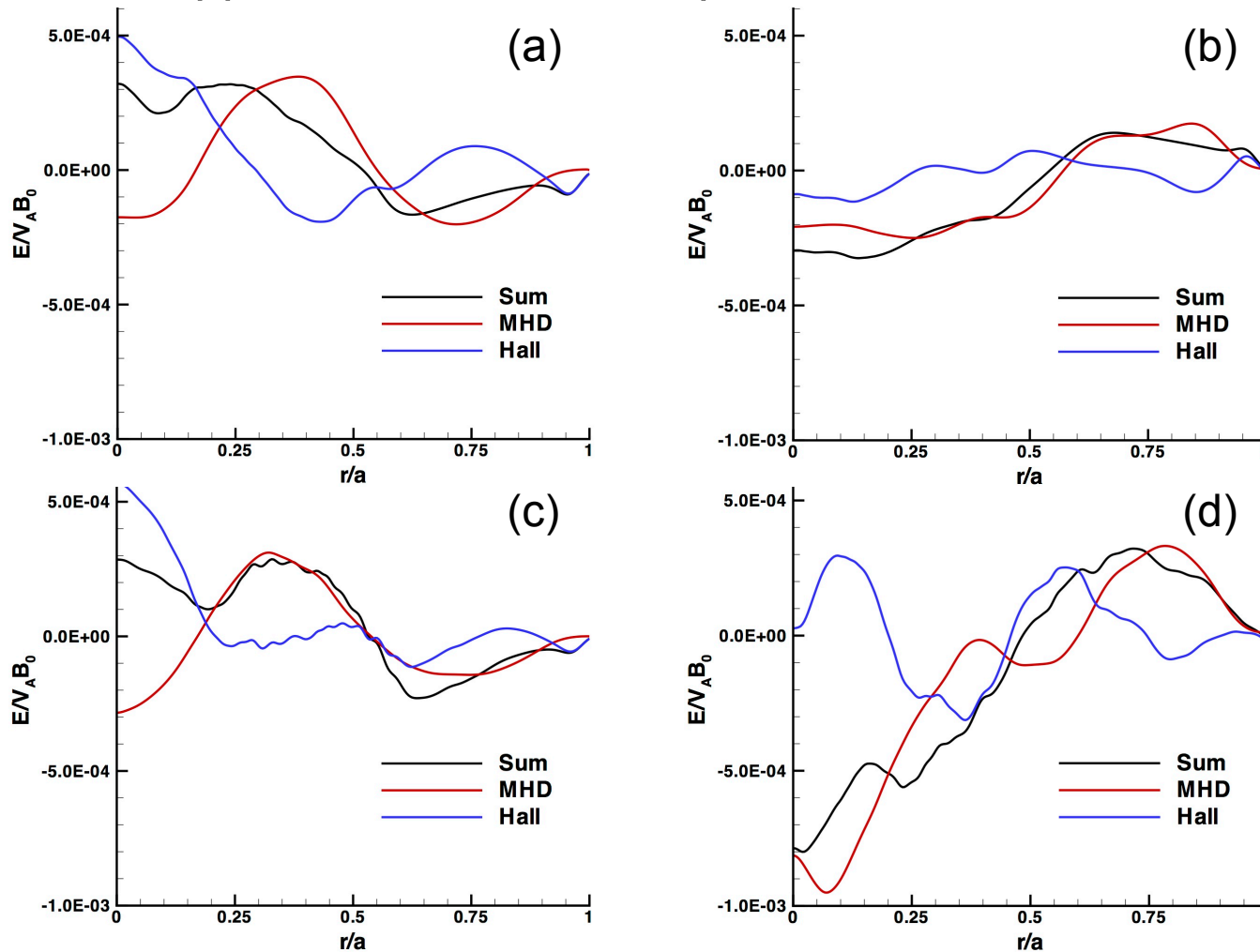
Evolution of reversal parameter ( $F$ ) and spectral width ( $N_s$ ) for positive current.



Evolution of  $F$  and  $N_s$  with negative current.

# Background flow alters Hall and MHD dynamo effects.

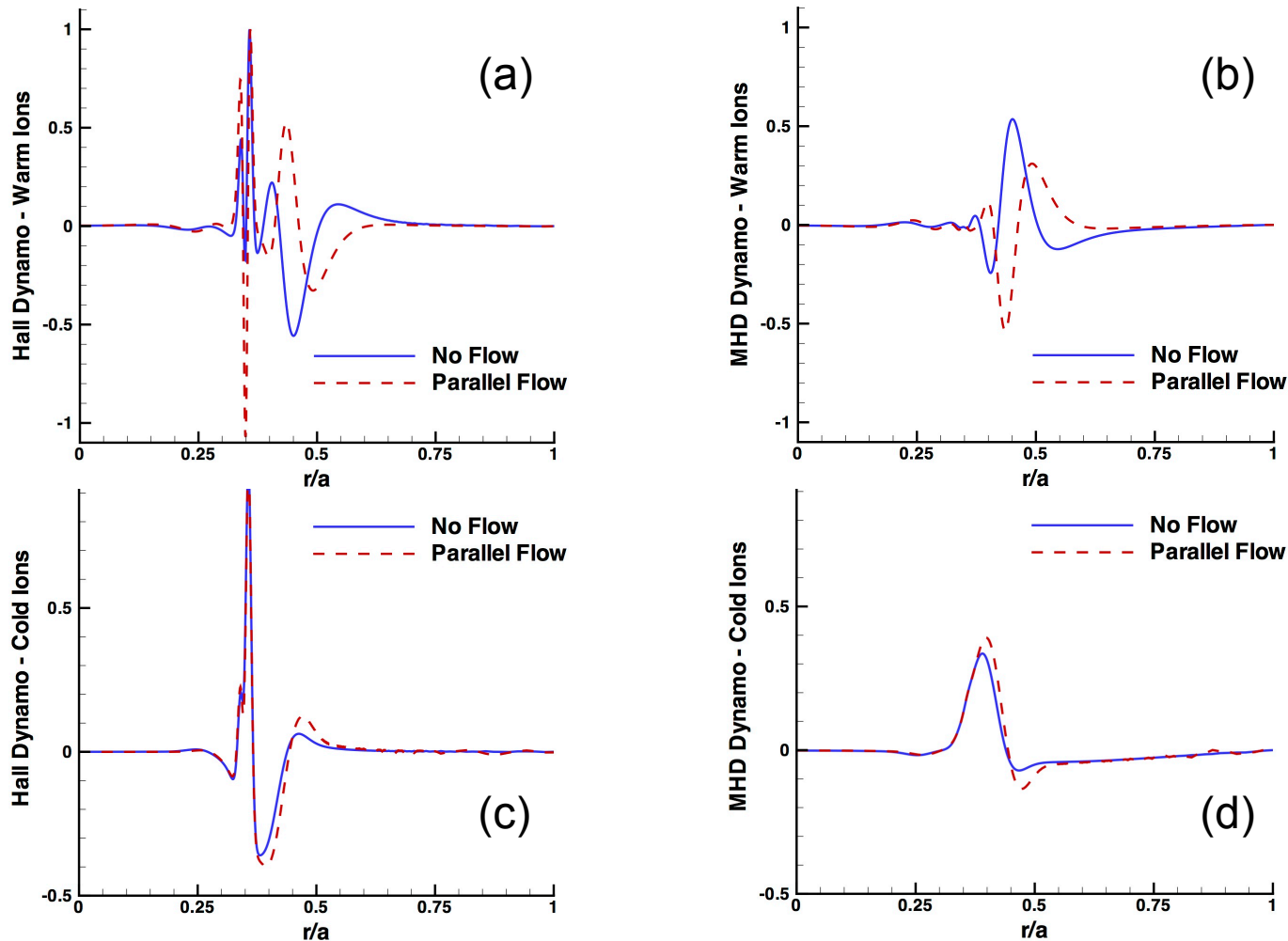
- At reversal the sum is similar for the two current orientations, but the contributions oppose each other with positive current.



Dynamo contributions at initial reversal with (a)  $J_0 \cdot B_0 > 0$  and (b)  $J_0 \cdot B_0 < 0$  and at greatest reversal with (c)  $J_0 \cdot B_0 > 0$  and (d)  $J_0 \cdot B_0 < 0$ .

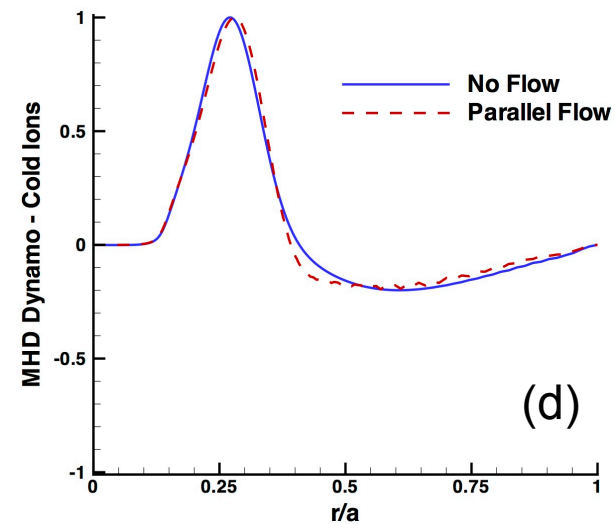
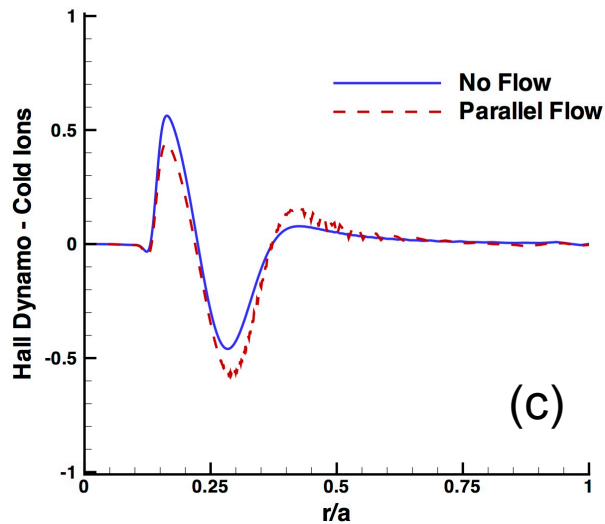
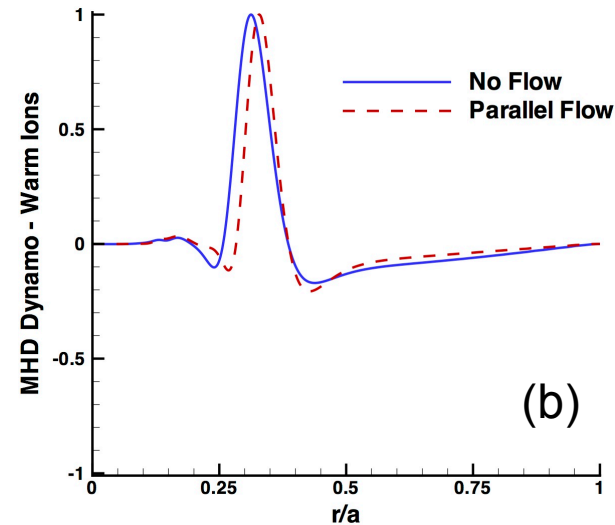
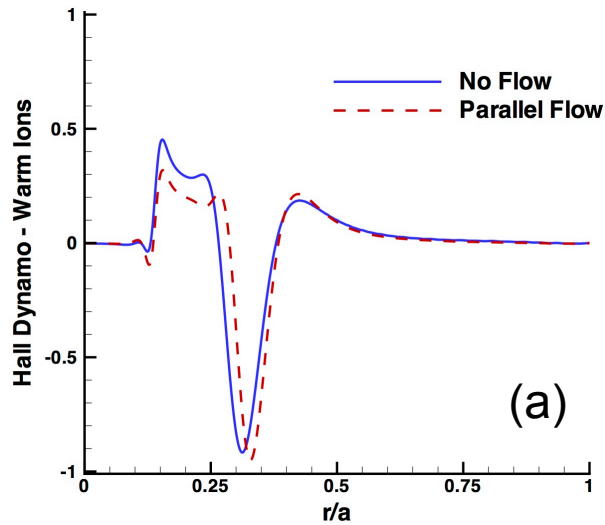
## Background flow also affects quasilinear dynamo.

- This set of quasilinear profiles is computed from linear tearing-mode ( $\Delta' = 48$ ) eigenfunctions for  $S=80,000$ ,  $Pm=0.1$ .



Dynamo effects from tearing-mode results with  $J_0 \cdot B_0 > 0$  (a) Hall with warm ions, (b) MHD with warm ions, (c) Hall with cold ions, (d) MHD with cold ions.

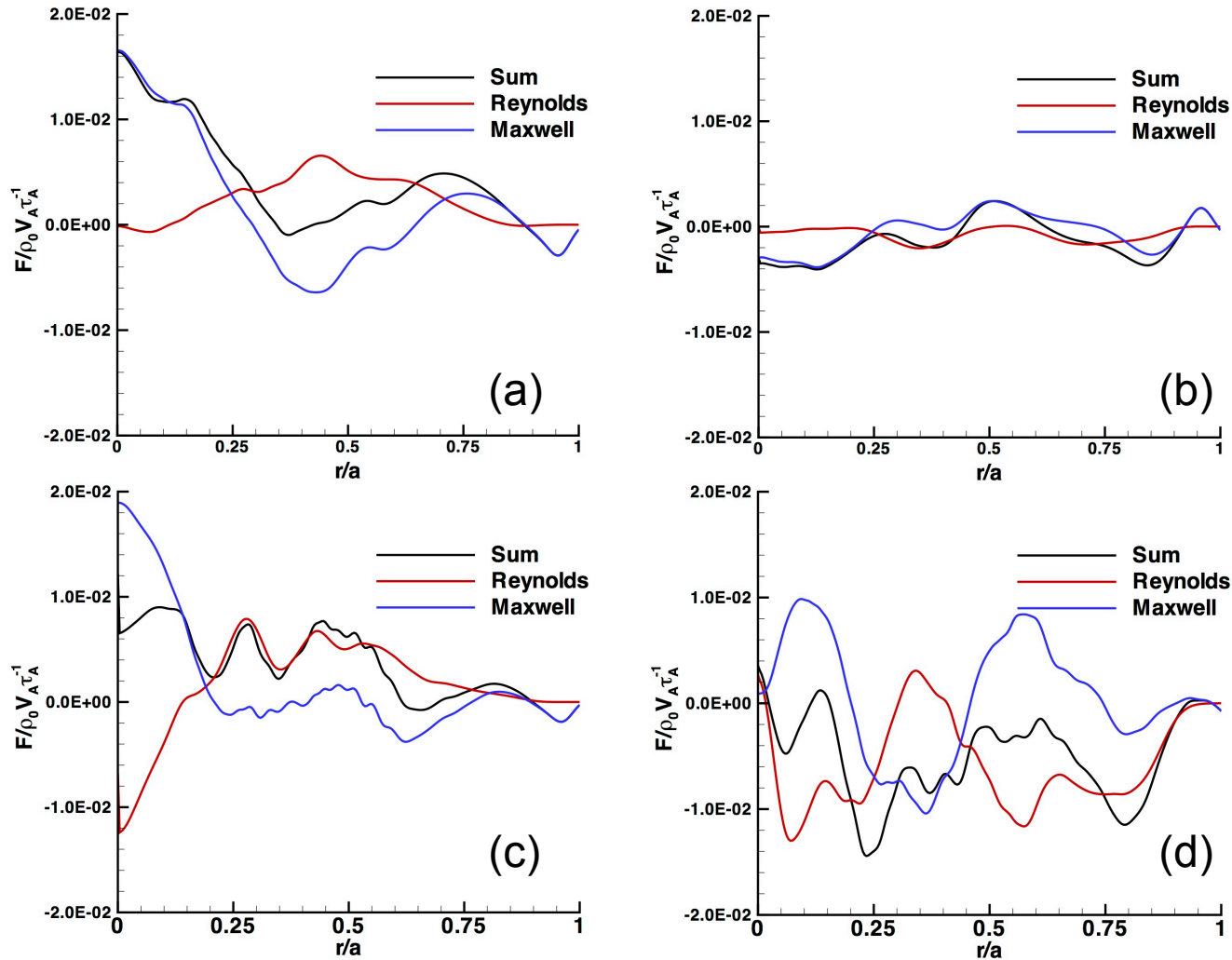
# Flow does not affect dynamo from ideal-unstable modes.



Dynamo effects from ideal-mode results with  $J_0 \cdot B_0 > 0$  (a) Hall with warm ions, (b) MHD with warm ions, (c) Hall with cold ions, (d) MHD with cold ions.

- Flow can change the sign of Hall & MHD dynamo from warm-ion tearing.

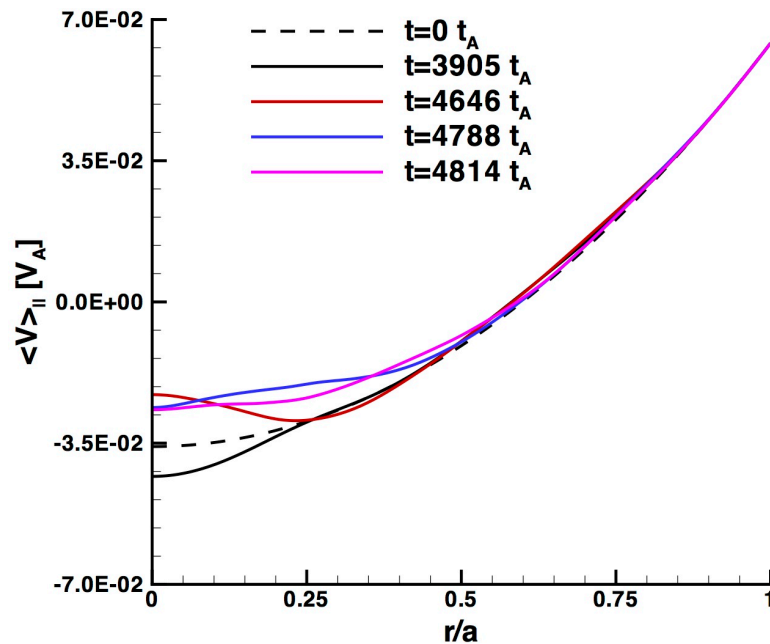
At reversal in the 3D cases, Maxwell-stress forces are stronger than Reynolds-stress forces for both  $\mathbf{J}_0$  orientations.



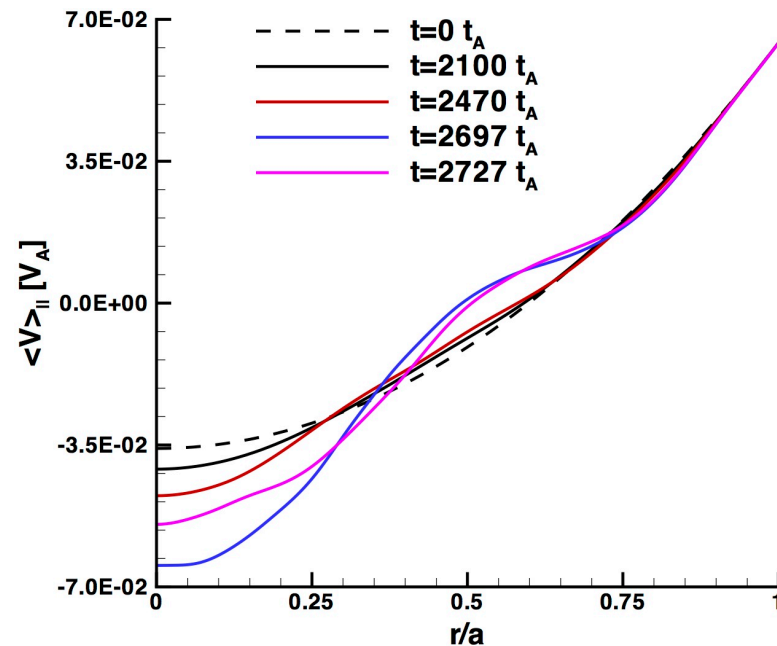
Fluctuation-induced parallel force-densities at initial reversal with (a)  $\mathbf{J}_0 \cdot \mathbf{B}_0 > 0$  and (b)  $\mathbf{J}_0 \cdot \mathbf{B}_0 < 0$  and at greatest reversal with (c)  $\mathbf{J}_0 \cdot \mathbf{B}_0 > 0$  and (d)  $\mathbf{J}_0 \cdot \mathbf{B}_0 < 0$ .

Although Reynolds-stress contributions increase by the time of peak reversal, sequencing is important for the parallel flow profile evolution.

- For both orientations, parallel flow evolves in the direction of  $\mathbf{J}_0$ , consistent with Hall dynamo relaxation of the current profile.



Evolution of the parallel flow profile with positive current.



Evolution of the parallel flow profile with negative current.

- In MST,  $\mathbf{J}_0 \cdot \mathbf{B}_0 < 0$ , and this two-fluid computation evolves flow in the opposite direction of the observations in Ref. [Kuritsyn, PoP **16**, 55903.]



# Conclusions

- First-order FLR modeling of warm ions produces  $\nabla B$  and poloidal-curvature drift-tearing effects in pinch profiles.
  - At large- $\rho_i$ , tearing decouples from ions, so ion kinetics may not be critical.
- Nonlinear island evolution in pinch profiles is influenced by ion FLR.
  - With cold ions, two-fluid saturation is equivalent to MHD.
  - When modeling experimentally relevant parameters with first-order FLR, warm-ion effects reduce island widths.
- Two-fluid multi-helicity simulations show non-MHD effects similar to those observed in MST: Hall dynamo and competition between Maxwell and Reynolds stresses.
- Background flows affect the profile evolution.
  - Both the Hall and MHD dynamo profiles differ from results without background flow.
  - Background flow breaks the symmetry between conditions with parallel and anti-parallel current.

# Future Work

- Investigate profiles with nonuniform background pressure.
  - Incorporates pressure-driven effects.
  - Changes the  $\rho_s$ -profile to decrease in  $r$ .
- Include parallel viscosity in the model.
  - Fluctuations in  $\hat{\mathbf{b}}$  and  $\nabla_{\parallel}\mathbf{V}$  can affect momentum transport.
- Investigate possible effects from the toroidal-field circuit.
- Apply the same modeling in toroidal geometry.